HHS Public Access

Author manuscript

J Neural Eng. Author manuscript; available in PMC 2023 November 29.

Published in final edited form as:

J Neural Eng. ; 18(5): . doi:10.1088/1741-2552/ac2bb8.

Wireless microelectrode arrays for selective and chronically stable peripheral nerve stimulation for hindlimb movement

Rebecca A Frederick[1], **Philip R Troyk**[2], **Stuart F Cogan**[1,*]

[1]Bioengineering Department, The University of Texas at Dallas, Richardson, TX, United States of America

[2]Biomedical Engineering Department, Illinois Institute of Technology, Chicago, IL, United States of America

Abstract

Objective.—Maximizing the stability of implanted neural interfaces will be critical to developing effective treatments for neurological and neuromuscular disorders. Our research aims to develop a stable neural interface using wireless communication and intrafascicular microelectrodes to provide highly selective stimulation of neural tissue.

Approach.—We implanted a wireless floating microelectrode array into the left sciatic nerve of six rats. Over a 38 week implantation period, we recorded stimulation thresholds and movements evoked at each implanted electrode. We also tracked each animal's response to sensory stimuli and performance on two different walking tasks.

Main results.—Presence of the microelectrode array inside the sciatic nerve did not cause any obvious motor or sensory deficits in the hindlimb. Visible movement in the hindlimb was evoked by stimulating the sciatic nerve with currents as low as 4.1 μA. Thresholds for most of the 96 electrodes we implanted were below 20 μA, and predictable recruitment of plantar flexion and dorsiflexion was achieved by stimulating rat sciatic nerve with the intrafascicular microelectrode array. Further, motor recruitment patterns for each electrode did not change significantly throughout the study.

Significance.—Incorporating wireless communication and a low-profile neural interface facilitated highly stable motor recruitment thresholds and fine motor control in the hindlimb throughout an extensive 9.5 month assessment in rodent peripheral nerve. Results of this study indicate that use of the wireless device tested here could be extended to other applications requiring selective neural stimulation and chronic implantation.

Keywords

wireless; peripheral nerve; stimulation; microelectrode array; rat sciatic nerve; hindlimb; chronic

*Author to whom any correspondence should be addressed. stuart.cogan@utdallas.edu.

Supplementary material for this article is available online

1. Introduction

Intraneural microelectrode arrays have long been studied as a means to maximize the selectivity and energy efficiency of stimulation in neural tissue. A variety of array designs have been developed for use in either cortex or peripheral nerve, with the most common designs being of the same type as the Utah array [1], Michigan probe [2], or transversal intrafascicular multichannel electrode [3]. Human trials have successfully utilized intraneural microelectrode arrays for recording in cortex [4] and stimulation in peripheral nerves [5]. However, maintaining long-term performance of all electrodes in an implanted device continues to be difficult to achieve. Most studies of intraneural arrays report a decline in recording or stimulation capabilities over time, and it is still not fully understood to what degree these changes are caused by various confounding factors such as the ongoing physiological response of the tissue to the implanted device [6], response of the tissue to applied electrical stimuli [7–9], properties of the electrode or device materials [5, 10], or physical damage to the implanted device or connecting wire cables [6]. And so, there is a continued need to investigate a variety of methods for improving long-term performance of intraneural microelectrode arrays that can address the various factors affecting stability of the device–tissue interface.

Our study assesses the long-term performance of a wireless intraneural array, the wireless floating microelectrode array (WFMA), by investigating selective recruitment of lower limb motion. As a self-contained wireless device, the WFMA eliminates the need for an implanted battery, cables, and percutaneous connector. We expect implementing the use of this wireless array would contribute to improving long-term performance of implanted intraneural devices by reducing the total number of hardware components (reducing the opportunity for components to break) and by eliminating tethering forces on the tissue caused by the presence of wire cables attached to the electrode array.

In this study, we use the rat sciatic nerve as a model for both functional and behavioral assessments. We investigated the motor response to stimulation as well as overall limb function following implantation of the WFMA into the healthy sciatic nerve of rodents. We investigated the current thresholds required for eliciting movement and the pattern of motion evoked by applying stimulation at individual electrodes. We also tracked animals' response to two different sensory stimuli, performance on a ladder walking task, and performance on a treadmill walking task to assess limb function before and after device implantation. We then tracked changes in limb function, current thresholds, and evoked movement patterns for a period of 38 weeks after device implantation to evaluate the chronic stability of the device–tissue interface.

2. Methods

All animal procedures were performed in accordance with the guidelines of the Institutional Animal Care and Use Committee of The University of Texas at Dallas.

2.1. Device design and assembly

The WFMAs were fabricated at the Illinois Institute of Technology using ceramic platforms supplied by MicroProbes for Life Sciences. The platforms from MicroProbes each comprised 16 Parylene-insulated (and 2 uninsulated reference and counter) iridium shaft electrodes connected to metal traces on the platform. The integrated circuit and RF telemetry coil were attached to the platform at the Illinois Institute of Technology by wire bonding and the electronics assembly encapsulated in silicone by vacuum casting. The iridium electrodes (2000 μm^2 surface area) were then electrochemically cleaned and activated to form an activated iridium oxide film (AIROF) [11, 12] using electrochemical cleaning and activation functions designed into the integrated circuit. Electrode shafts had alternating lengths of 1150 μm and 1350 μm with 400 μm spacing center-to-center. The silicone cuff has a 500 μm thick wall and base, making the electrode lengths available for insertion 650 μm and 850 μm. The completed WFMA with silicone nerve guide, electrode layout, and implanted device orientations are shown in figure 1. Reverse telemetry is transmitted at 145 kHz using the NeuroTalk™ interface and frequency shift keying (FSK) modulation of a Class-E converter. Forward commands are transmitted at 1.1 Mbits s^{-1} and WFMAs are wirelessly powered at 4.5 MHz. Further details on the design and manufacture of WFMAs can be found in prior research describing the telemetry coil [13, 14–16], application specific integrated circuit (ASIC) [17], electrodes [11, 18], and stimulation method [19].

2.2. Device implantation

One WFMA device was implanted in each of $n = 6$ female Sprague Dawley rats at 10–16 weeks of age, after devices were sterilized with ethylene oxide. Inhaled isoflurane at 2.0%–3.0% was used to anesthetize the animal and the left hindlimb was shaved and cleaned with 70% alcohol, 10% povidone-iodine, and again with 70% alcohol. Opthalmic ointment was placed over each eye to prevent corneal drying during anesthesia. An incision was made in the skin parallel and approximately 1 cm caudal to the femur. The biceps femoris muscle was separated from gluteus superficialis and vastus lateralis muscles by spreading the connective tissue between the muscles. No incisions were made in the muscle tissue. Biceps femoris was then retracted to reveal the sciatic nerve. To prepare for device implantation, connective tissue was separated from the entire circumference of the left sciatic nerve proximal to the branching of the tibial, peroneal, and sural nerves. Connective tissue was separated without damaging any visible cutaneous branches from the nerve until approximately 1.2 cm was exposed along the length of the nerve.

The nerve was gently lifted using a custom-made glass hook, and the WFMA was placed under the exposed nerve section so that the flat coil surface rested on the underlying muscle tissue and the electrodes pointed towards the nerve. The nerve was then placed inside the silicone channel, and the nerve and WFMA device were carefully pressed together until the electrodes penetrated the sciatic nerve. After removing fluid from the edges of the silicone channel, the device was secured in place using a silicone sealant (Kwik-Cast™) that cures at body temperature and adheres to the silicone channel without attaching to the surrounding tissue. Care was taken to ensure the sealant did not enter the channel and contact (occlude) the electrodes. Devices were implanted with alternating orientations, such that the row of five electrodes was positioned to the left (towards the cranial direction) for $n = 3$ animals

(A01, A03, and A05) and to the right (towards the caudal direction) for $n = 3$ animals (A02, A04, and A06). Figure 1 (bottom, right) shows an implanted WFMA device after it was secured with silicone sealant (green). Table 1 summarizes animal subject identifiers and the device identifier with implant orientation for the six rats implanted with a WFMA.

To confirm device function prior to closure of the surgical site, the reverse telemetry feature of the WFMA was used to record voltage transients in response to 4.7 μA, 200.2 μs current pulses (~1 nC ph^{-1}, 50 μC cm^{-2}) at 50 Hz frequency. In two animals (A01 and A04), testing revealed that the silicone sealant was in contact with the uninsulated counter electrode, interfering with current flow and device operation. The sealant was carefully removed, the device repositioned on the nerve, and new sealant was placed over the channel. Repeated voltage transient recordings showed normal operation of both devices. Once the implanted device was confirmed to be functioning as expected, the separated muscles were closed with 4–0 silk suture and the skin closed with 11 mm suture clips. Animals were given slow-release buprenorphine immediately after surgery and again 72 h after the procedure to manage post-op pain. As a prophylactic, animals were given cefazolin antibiotic immediately after surgery and water with sulfamethoxazole ad libitum for one week after the implantation procedure. The success rate for device implantation was 100%, where implantation is considered successful if the animal has no complications recovering from anesthesia, there are no postoperative infections, and reverse telemetry immediately after implantation within the nerve confirms normal device function.

2.3. Functional assessments

Overall function of the hindlimb was assessed for (a) response to nociceptive mechanical stimulus [20] using a dynamic plantar aesthesiometer (Ugo Basile®, Gemonio Italy), (b) response to nociceptive thermal stimulus [20] using a plantar test Hargraeve's apparatus (Ugo Basile®, Gemonio Italy), (c) proprioception changes using the horizontal ladder walk test, and (d) motor function using constant-speed treadmill walking trials. All functional assessments were completed one week before device implantation to collect baseline data. Functional assessments were repeated once per week after device implantation starting on post-op week 1 (day 7) and continuing through postop week 10. After week 10, assessments were repeated once every two weeks from post-op week 12 through week 38. Functional assessments were completed for the $n = 6$ animals with implanted WFMAs as well as a control group of $n = 6$ age-matched animals (female Sprague Dawley rats B01, B02, B03, B04, B05, and B06).

The mechanical stimulus was applied to the plantar surface of the rear paws using a Von Frey-type 0.5 mm filament (figure 2(f)) with an automated ramp-up to a maximum force of 50 *g* over 20 s. The thermal stimulus was applied to the plantar surface of the rear paws using infrared light. Twelve trials were completed for each of the two assessments (mechanical and thermal), with six trials completed for each of the two rear paws (right and left). Experimental setup for thermal and mechanical stimuli assessments is shown in figure 2 panels (d) and (e), respectively.

Each ladder walk trial was video recorded and each step was scored on a scale of 0–6 using the methods described in [21]. Each step was given a score from the following

categories: 0—total miss, 1—deep slip, 2—slight slip, 3—replacement, 4—correction, 5—partial placement, 6—correct placement. A uniform pattern of 100 rungs with 1 cm spacing was used in every testing session (figure 2(a)). Animals were also recorded walking one of 17 randomized patterns of ladder rungs in each testing session starting at post-op week 2 to control for animals learning the uniform pattern and potentially improving their task performance over time. The only restriction imposed on the random pattern was that the distance between any two rungs must be equal to or less than 4 cm. In each testing session, four trials were recorded for each pattern of ladder rungs for each animal.

Treadmill walking sessions were completed after ladder walking trials. Animals were first placed on the clear belt and images were taken of the underside of the paws while the animal was at rest for toe spread measurements. Each walking trial was video recorded (figures 2(b) and (c)) while animals walked continuously for at least 1 min with the belt speed set at 7.0 cm s^{-1}. One background video was recorded at the end of each session with no animal on the treadmill, to capture any variations in lighting or camera position over the 38 week study.

2.4. Neural stimulation and tracking limb motion

Stimulation trials were performed under anesthesia (isoflurane 1.0%–2.0%) once per week starting at post-op week 1 (day 9) and continuing through post-op week 8. Testing sessions then continued once every two weeks for post-op week 10 through week 38. We expect the level of anesthesia used during stimulation trials would have no effect on direction of limb movement, and minimal effect on current thresholds for eliciting motor response [22] while allowing animals to comfortably undergo extended testing sessions. Each testing session was limited to a maximum of 2 h to avoid any potential complications related to repeated and prolonged periods under anesthesia. Animals were positioned on an elevated surface such that the left hindlimb was hanging and free to move without restriction, and opthalmic ointment was placed over each eye. Two Stingray F033C IRF CSM video cameras (Allied Vision Technologies GmbH, Germany) were positioned to view the lateral and dorsal surfaces of the foot and track movement of the left hindlimb.

The wireless telemetry coil was then positioned over the implanted device, near the hip joint. After confirming signal transmission, voltage transients were recorded at 4.7 μA, 200.2 μs, and 50 Hz to confirm each electrode exhibited a typical transient response (i.e. resistive voltage drop at the start of the pulse followed by electrode charging) and not a large resistive voltage drop indicative of a broken electrode. Each electrode was then tested one-at-a-time using 200.2 μs pulses at 1 Hz, gradually increasing the current until a 1 Hz twitch was observed in the left paw that was clearly distinguishable from motion of the animal due to breathing. Video of limb motion was then recorded at the threshold current for generating a visible twitch (I_{th}) and at two or more current values above threshold. Primary limb motion in each recording was classified as plantar flexion, dorsiflexion, or digit motion only. Secondary limb motion evoked by stimulation, if present, was recorded as inversion, eversion, abduction, adduction, supination, pronation, toe flexion, toe extension, or single digit movement (usually digit one or five). Experimental setup for the stimulation tests is shown in figure 2, panels (g) through (i).

2.5. Stimulation in awake animals

On the final day of the study, one additional stimulation session was performed on awake animals while unrestrained inside their housing cage to determine if stimulation with the WFMA caused pain or discomfort for the animals. The grimace scale [23] was used to score animal behavior during each applied stimulus and determine if the stimulus caused pain. The awake stimulation session was performed before anesthetizing the animal for week 38 data collection on stimulation thresholds and movement directions. The external telemetry coil was held against the left hip while the animal was stationary (but free to move) within its cage and communication with the device was confirmed before applying five pulses at 200.2 μs and 1 Hz at three different amplitudes: below I_{th} (3.4–19.6 μA), at I_{th}, and above I_{th} (no greater than I_{th} + 10 μA) using I_{th} recorded during the previous test session (week 36). Electrodes that did not evoke movement during the previous test session and so did not have a recorded I_{th} were tested at one amplitude of 10.2 μA during the awake stimulation session. At the time of the awake stimulation session, it was not possible to determine exactly why electrodes did not evoke movement in the previous week, e.g. due to a change in electrode location, a change in physiological response, or damage of the electrode material. And so, an amplitude of 10.2 μA was chosen so that electrodes would not be excessively polarized to the point of causing damage to the surrounding tissue if the electrode did not evoke movement during the previous session due to damage to the activated iridium oxide film.

The process of applying five pulses each at 10.2 μA or at three different amplitudes was repeated for each of the 16 electrodes, one at a time. Two electrodes were chosen for testing additional current amplitudes: one that did not evoke motion during the previous session or throughout the study, and one that consistently evoked motion throughout the study. The electrode that did evoke motion was tested at 2–3× I_{th} to evoke a strong muscle contraction and assess the animal's response. The electrode that did not evoke motion was tested up to 60 μA to assess the animal's response when applying current amplitudes above the I_{th} range for most electrodes (4.1–40.0 μA). Animals were allowed to recover for 30 min before beginning anesthesia for the final stimulation session of the study.

2.6. Data analysis and statistics

Data for response to mechanical stimulus and thermal stimulus were first processed to remove outliers. For mechanical stimuli, an outlier was defined as any data point where the ratio of the recorded force value to time value was more than 0.3 g s^{-1} higher or lower than the expected ratio of 2.5 g s^{-1} set by the applied ramp of 50 g over 20 s. One exception is values where the stimulus reached the maximum value of 50 g, where the time value may extend beyond 20 s before the animal withdraws the paw. The set threshold of ratio values less than 2.2 g s^{-1} or greater than 2.8 g s^{-1} were chosen so that good trials (with correct probe placement and the animal in a resting state) where the force value reached 50 g were not excluded. For thermal stimuli, an outlier was defined as any value greater than 3.0 standard deviations from the median value of all data points (equivalent to valuesgreaterthan12.89s). Values outside this threshold were found to correspond to trials where there was insufficient recovery time between heat application at the same paw or incorrect placement of the infrared source under the paw.

Data from ladder walking trials were compiled to determine the total number of steps, average step score for each foot, a count of missed steps, and percentage of 'normal' versus 'missed' steps for each testing session. A missed step was defined as any step scored as 0, 1, or 2 and a normal step was any step scored as 3, 4, 5, or 6. Each video from treadmill walking trials was analyzed using TreadScan (CleverSys Inc., Reston, VA, USA) to determine the average step length, step time, stance time, and swing time of the left and right hindlimbs.

Data for mechanical and thermal stimuli as well as ladder and treadmill walking trials were assessed using regression analysis (GraphPad Prism 7). Regression analysis was performed across all reported time points for paw withdrawal time—heat, paw withdrawal time—pressure, percent missed steps, stride length, and stride time. Each animal and foot combination were assessed separately (implanted group—rear left, implanted group—rear right, control group—rear left, and control group—rear right).

3. Results

3.1. Electrode locations

During implantation we found that the WFMA electrode array layout (originally designed for cortical implantation) was wider than the sciatic nerve diameter at the time of implantation due to the 400 μm center-to-center spacing between electrodes. Over all six implanted animals, this resulted in a group of 21 electrodes located at the outer edge of the nerve, corresponding to one electrode row (of either 4 or 5 electrodes) for each animal that was located at the right side of the nerve (when viewed from above). Figure 3 shows gross position of the implanted electrodes after conclusion of the 38 week study from a top-down view into the silicone guide channel. Images were taken after fixation of the whole tissue sample with the WFMA device in-place, removal of tissue encapsulation around the nerve and device, and removal of the green silicone sealant used to keep devices from migrating after implantation. After recording the images shown, each device was separated from the nerve for further analysis of both the WFMA and sciatic nerve tissue. Figure 4 shows selected examples of gross position of implanted electrodes from a side view into the silicone guide channel. Representative comparisons of the same row of electrodes are shown for the device removed from animal A04 (figure 3 bottom center and figure 4 left) and animal A06 (figure 3 bottom right and figure 4 center) shows that electrode tips are more superficial within nerve tissue for animal A04 than A06.

3.2. Functional assessments

Paw withdrawal times in response to mechanical and thermal stimuli did not significantly change over time for the implanted limb or any controls. Variability in the data from week-to-week appear to be accounted for by subject-to-subject differences. Figure 5 shows paw withdrawal response times for thermal and pressure stimuli recorded pre-op and post-op at weeks 1, 2, 4, 8, 16, 28, and 38. Regression analysis of paw withdrawal time versus study week did not find any trend in the data, as the best fit model was a line with near-zero slope. Best-fit slopes (seconds per study week) calculated for response to heat were: −0.025for implanted group, left; −0.005 for implanted group, right; 0.035 for control group, left; 0.013

for control group, right. Best-fit slopes (seconds per study week) calculated for response to pressure were: −0.027 for implanted group, left; −0.027 for implanted group, right; 0.031 for control group, left; −0.009 for control group, right.

For the ladder walking task, no deficits were observed for implanted animals at any of the reported time points. As expected, animals in both implanted and control groups performed slightly better on the task over time (less errors, higher average step score) for the uniform rung pattern and performed slightly worse (more errors, lower average step score) on the random rung patterns at each time point. Overall, error rates were less than 5% and average step scores were between 5 and 6. Figure 6 shows the percentage of missed steps (scores 0–2) and table 2 lists average step scores over time for the right and left hindlimb in each of the animal groups (implanted and control) for both the uniform and random patterns of ladder rungs. Regression analysis of the percent of steps missed versus study week did not find any trend in the data, as the best fit model for each data set was a line with near-zero slope. Best-fit slopes (percent of steps per study week) calculated for steps missed were: −0.013 (uniform) and −0.066 (random) for implanted group, left limb; −0.021 (uniform) and −0.063 (random) for implanted group, right limb; −0.002 (uniform) and −0.011 (random) for control group, left limb; −0.011 (uniform) and −0.049 (random) for control group, right limb.

For the treadmill walking task, no deficits were observed for implanted animals at any of the reported time points. Average time in stance versus swing for each step was within expected values, where time in stance comprised 77.6 ± 1.6% and 77.0 ± 1.7% of total step time for control group animals' rear left and rear right limbs, respectively, and 75.9 ± 1.9% and 74.8 ± 1.8% for implanted animals' rear left and rear right limbs, respectively. Figure 7 shows step length and total step time averages for the right and left hindlimb in each animal group. Regression analysis of step length versus study week did not find any trend in the data, as the best fit model for each data set was a line with near-zero slope. Best-fit slopes (millimeters per study week) calculated for step length were: 0.020 for implanted group, left limb; 0.112 for implanted group, right limb; 0.083 for control group, left limb; −0.019 for control group, right limb. Regression analysis of step time versus study week found total stride time increases from pre-op to post-op week 38. Best-fit slopes (milliseconds per study week) for step time were: 2.395 for implanted group, left limb; 2.115 for implanted group, right limb; 2.159 for control group, left limb; 1.716 for control group, right limb.

3.3. Response to stimulation

Partial data from weeks 1 through 8 of this study were also reported in [24]. Of the 96 electrodes implanted in total (16 electrodes per device in $n = 6$ animals), 21 appeared to be either within the epineurium or outside the nerve upon visual inspection at the time of implantation (A01, A03, and A05—E14, E15, and E16; A02, A04, and A06—E01, E02, E03, and E04). Eleven of these 21 electrodes did not evoke a visible motor response at any point during the study period when tested up to the maximum current available from the WFMA (~86 μA). The remaining 10 electrodes in the group of 21 electrodes evoked a motor response sporadically over the 38 week study and at current thresholds typically above 40 μA.

We observed consistent motor recruitment patterns over a 38 week study period at thresholds ranging from 4.1 μA (0.8 nC ph^{-1}, 41 μC cm^{-2}) to 84.6 μA (16.9 nC ph^{-1}, 846 μC cm^{-2}). Electrodes located in rows at the center of the nerve typically had much lower motor activation thresholds (16 ± 9 μA, minimum 3.4 μA) than those at the outer edges of the nerve (39 ± 16 μA, minimum 10.2 μA). Our targeted movements, plantar flexion and dorsiflexion, were evoked by stimulation at one or more electrodes for each of the six implanted devices. The movement evoked by each electrode did not change for any testing session in the 38 week study period for 92 of the 96 electrodes.

3.3.1. Evoked limb motion—Selected examples of different movements evoked during stimulation sessions can be found in the video included in supplemental information (available online at stacks.iop.org/JNE/18/056058/mmedia). Figure 8(a) shows color maps of movements observed for all six animals for weeks 1 through 38 after device implantation. The color of each box indicates the type of primary movement evoked at the ankle, while overlayed symbols indicate evoked motion of the digits. Gold shading indicates overall planar flexion, with darker shading indicating supination. Blue shading indicates overall dorsiflexion, with lighter shading indicating pronation. In all color maps, white shading without symbols indicates no motor response was observed when the electrode was tested up to the maximum output of the device, data was not recorded at that time point, or the electrode was on functional when voltage transients were recorded at the time of device implantation, and so no further testing was performed on that electrode. Only electrode A01—E10 appeared to be non-functional based on voltage transients recorded at the time of device implantation. Recruitment patterns for animals A03, A04, A05, and A06 were consistent with expected recruitment of plantarflexion versus dorsi flexion based on anatomy of the rat sciatic nerve, spatial arrangement of the microelectrode array, and implanted device orientation. Recruitment patterns for animals A01 and A02 may have been affected by rotation of the sciatic nerve caused by methods used for the implantation procedure.

3.3.2. Stimulation thresholds—The total number of implanted electrodes generating visible movement ranged from 66 (68.8%) to 79 (82.3%) across all recorded timepoints. The number of electrodes with I_{th} below 20 μA ranged from 45 (68.2% of electrodes evoking movement, 46.9% of 96 total electrodes) to 64 (87.7%, 66.7% of total) throughout the 38 week study period. I_{th} for electrodes evoking dorsiflexion was generally lower than those evoking plantar flexion. Across all animals and timepoints, dorsiflexion electrodes had an I_{th} range of 3.4–69.1 μA with an average and standard deviation of 14.7 ±2.6 μA while plantar flexion electrodes had an I_{th} range of 5.4–60.9 μA with an average and standard deviation of 16.6 ± 1.2 μA. Figure 8(b) shows all threshold values recorded for all electrodes in all $n = 6$ animals at all timepoints. The color map indicates what threshold range the value was within: dark blue = less than 20 μA, gold = 20–40 μA, light blue = greater than 40 μA. An “x” is used to indicate values less than 10 µA or greater than 60 μA (where maximum device output is ~86 μA). Figure 8(c) shows threshold values over time for each implanted electrode in one animal (A02) with an inset showing location of the electrode within the array layout. In figure 9, we provide a break-down of the total number of electrodes generating movement in the limb and the associated threshold values required

throughout the study in order to further assess changes in the device-tissue interface over time.

4. Discussion

This chronic 38 week study extends earlier studies of WFMA stimulation of rat sciatic nerve [25, 26] to include a larger cohort of implanted animals and behavioral testing to assess deficits that might result from the presence of devices chronically on the nerve. We were able to demonstrate selective motor recruitment in the rat hindlimb using a fully wireless implanted stimulator connected to an array of 16 microelectrodes inserted into the rat sciatic nerve, just proximal to the nerve's point of branching into tibial, peroneal, and sural nerves. Behavioral testing showed no observable changes in the animals' ability to sense heat or pressure stimuli, nor their ability to perform a ladder walking motor task. No evidence of pain or discomfort (as assessed by the grimace scale) was observed following device implantation for any animal throughout the study. Additionally, none of the six implanted animals demonstrated behaviors associated with pain or discomfort during stimulation tests performed on the final day of the study while the animal was awake and unrestrained within its cage. Based on reports of trials in humans with similar devices [5], we expect these devices could be appropriately scaled in size and translated to human use without significant negative effects related to device implantation. Modifications that could be made to the WFMA include the size of the telemetry coil, spacing and length of the electrode microwires, and geometry of the silicone nerve guide channel to accommodate a larger diameter nerve and better target the anatomy and fascicular structure of the human sciatic nerve.

The arrangement of electrodes recruiting plantar flexion versus dorsiflexion was generally consistent with expected recruitment based on published topography and fascicular organization of the rat sciatic nerve [1, 27] and spatial arrangement of the electrode array. We expect most electrodes will evoke plantar flexion as the tibial nerve fascicle occupies a larger proportion of the sciatic nerve than the peroneal nerve fascicle. For devices implanted in the C-R orientation, we expect electrode rows E01-E04 and E05-E08 would be most likely to evoke dorsiflexion, while in the C-L orientation dorsiflexion recruitment is most likely with electrode rows E16-E14 and E09-E13. We observed expected recruitment patterns for animals A03 and A05 (C-R orientation) and A04 and A06 (C-L orientation). Recruitment patterns for animals A01 and A02 were not as expected and may have been influenced by slight rotation of the sciatic nerve caused by the implantation procedure. A glass hook was used to place the nerve inside the silicone guide channel, before inserting the electrodes, and we observed some rotation of the nerve when manipulating the glass hook to release the nerve into the guide channel. Mapping patterns of stimulation-evoked movements showed that electrodes that were located in the same row of the microelectrode array and were the same length (650 or 850 μm) typically evoked the same direction of paw movement. Electrodes within the same row should be located within the same fascicle along the length of the nerve, barring any major differences in depth of penetration, and so this finding was consistent with expected performance for this type of intrafascicular microelectrode array.

An unexpected finding of this study was the variety of nuanced movements of the paw we observed during stimulation. Video recordings showed many instances and varieties of single digit movements, ankle rotation about multiple axes, and flexion or extension of all digits either alone or coupled with ankle rotation. The use of small surface area (2000 μm^2) intrafascicular electrodes resulted in recruitment thresholds below 20 μA (4 nC) which likely facilitated the fine motor control achieved in this study. The stability and amplitude of motor recruitment thresholds for the WFMA penetrating electrode array is presumed to be highly dependent on ensuring that the electrodes are inserted within the fascicles of the nerve. For example, it can be seen in figure 8 (bottom) that electrodes in the two rows within the center of the array (E05-E08 and E09-E13) generally have more instances of motor recruitment and I_{th} values that are more stable over time. Electrodes in the two rows on the edge of the array (E01-E04 and E14-E16) show more variability in I_{th} values over time, presumably due to their location relative to fascicles within the nerve. Electrode 10 initially evoked plantarflexion at I_{th} = 10–15 μA, then I_{th} increased to above 60 μA at week 8, stopped evoking movement during weeks 10 and 12, then evoked dorsiflexion at I_{th} values below 20 μA at week 14 and for the remainder of the study, suggesting the location of the electrode relative to sciatic nerve fascicles may have changed during the implantation period.

In comparison to prior work, our results show similar selectivity and threshold ranges found in studies of wired intrafascicular arrays while studies of nerve cuff arrays have shown the ability to selectively recruit single muscles, but typically with higher threshold requirements. The wired high density Utah (intrafascicular) array reported motor recruitment thresholds of 1–100 μA in cat sciatic nerve with most electrodes in the 1–20 μA range [28, 29] and evoked selective ankle plantar flexion and dorsiflexion with constant-voltage stimulation in rat sciatic nerve using sputtered iridium oxide film (SIROF) electrode pairs with 208 μm tip-to-tip spacing [1, 30]. Flat interface nerve electrode (FINE) and other cuff electrode (extraneural) arrays have reported selective recruitment of single muscles with motor recruitment thresholds of 4–35 nC in human radial, ulnar, median and axillary nerves [31], 10–60 nC in human femoral nerve [32, 33], and 2–160 nC in human peroneal and tibial nerves [34, 35]. To our knowledge, no prior work reports the single digit recruitment in rat sciatic nerve that we observed during stimulation trials with the WFMA. It is possible other intrafascicular devices could evoke such movements, but the type of recruitment either was not looked for or simply was not included in the reported study results. It would be interesting to directly compare selectivity of wired intrafascicular arrays, wireless intrafascicular arrays, and wired cuff electrode arrays while applying the same stimulus to the same nerve.

Both Utah and FINE arrays have demonstrated neural stimulation or recording for more than one year in a small number of human subjects [5, 35, 36]. However, wired arrays have typically shown high failure rates in terms of percentage of electrodes able to perform desired stimulation or recording as the duration of implantation time increases. Cabling and interconnects are a frequent failure point in chronically implanted stimulation devices [6] and associated tethering forces can exacerbate the foreign body response in neural tissues, further compromising the ability to record or stimulate neural activity [37]. In one study of wired FMAs implanted in rat sciatic nerve [38], the five implanted devices failed at

6–13 weeks after implantation (where device failure was defined as all electrodes having a measured impedance greater than 2.0 MΩ).

Future studies could greatly benefit from the level of fine motor control we observed with the WFMA and could exploit the stability of the WFMA to further investigate effects of modulating pulse width, frequency, current amplitude, pulsing patterns, or other aspects of the applied stimulus. Many abnormal gait patterns after stroke are linked to dysfunction in the muscle groups controlling plantar flexion and dorsiflexion movements of the ankle [39]. And so, one potential application for the WFMA would be used as a completely implanted, wireless nerve stimulator for modulating plantar flexion and dorsiflexion in patients with chronic gait dysfunction following stroke.

Without the use of guided insertion or targeting more precisely than is possible using typical surgical techniques utilizing gross anatomical landmarks, we were able to place electrodes and evoke movement with more than 68% of the 96 implanted electrodes at all time points. Further, we were able to recruit targeted plantar flexion and dorsiflexion in all six animals in the study in addition to multiple secondary movements that were dependent on electrode location and stimulus amplitude. Due to the high percentage of electrodes generating a motor response, we believe that a majority of the implanted electrodes were located close to motor fibers within the sciatic nerve. Our observation that electrodes located in rows at the outer edge of the nerve generally had higher thresholds (when able to evoke movement) than electrodes located towards the center of the nerve further suggests that proximity of electrodes to motor axons in the sciatic nerve is the primary factor affecting threshold range for recruiting movement at the ankle. In future work we plan to report approximate electrode locations with respect to the fascicular structure within the nerve using micro-computed tomography and standard histological analysis of sciatic nerve samples collected from each implanted animal [40].

Based on our observations at the time of implantation surgery and threshold data, it is clear that the geometric pattern of electrodes on the WFMA platform is slightly too wide in the transverse direction of the nerve, and that some electrodes on each array were extraneural. Therefore, in subsequent studies targeting rat sciatic nerve, the transverse center-to-center electrode spacing of the WFMAs should be reduced in order to improve chances of successfully implanting all electrodes within a nerve fascicle without the need for additional guidance during insertion. Currently the electrode-to-electrode spacing is 400 μm. From initial histologic studies of explanted nerves from the implanted animal cohort in this study and from published histology [27], a spacing of 250–350 μm seems optimal. We expect reducing the spacing would not greatly impact ability to achieve fine motor control with the WFMA, as the implantation procedure alone resulted in noticeable differences in electrode locations among implanted animal subjects. However, the effect of electrode spacing on response to stimulation with multiple electrodes at the same time would need to be investigated in future work.

Overall, the WFMA devices demonstrated consistent performance within the operational range of the stimulator over the 38 week implantation, with only one electrode out of 96 that was non-functional as determined by voltage transient recordings provided by reverse

telemetry capabilities of the WFMA [25]. Further, as shown in figure 8, current thresholds and the recruited movements remained notably consistent over 38 weeks. Likewise, the number of electrodes exhibiting current thresholds below 20 μA remained at or above 55% of the total number of electrodes implanted for the duration of the study. We speculate that one major factor in achieving consistent functional stability is the wireless interface that avoids the need for cabling to the WFMA.

5. Conclusion

No obvious motor or sensory deficits were caused by implanting WFMAs with intrafascicular electrodes in a healthy sciatic nerve, or by short-duration stimulation of each electrode during weekly and bi-weekly testing sessions. Small movements of the limb were visible with currents as low as 4.1 μA, and thresholds for most of the 96 electrodes we implanted were below 20 μA. Knowledge of the fascicular structure of the sciatic nerve and careful device implantation allowed us to achieve predictable recruitment of plantar flexion and dorsiflexion using the WFMA. This study demonstrated that WFMAs provide a stable nerve interface that can achieve highly selective control of limb motion. Where motor recruitment patterns and thresholds did not change significantly throughout an extensive 9.5 months of testing.

Supplementary Material

Refer to Web version on PubMed Central for supplementary material.

Acknowledgments

The authors would like to recognize and thank the team of students who made significant contributions to data collection efforts for the study: Angela Abraham, Lasya Priya Anand, Emily Baumbach, Kayla Caughlin, Ananya Kumaresh, Maryam Mohammad, Afza Mohammed, Nihitha Nukala, and Adiva Sahar.

Data availability statement

The data that support the findings of this study are available upon reasonable request from the authors.

References

[1]. Wark HAC et al. 2013 A new high- density (25 electrodes/mm2) penetrating microelectrode array for recording and stimulating sub-millimeter neuroanatomical structures J. Neural Eng. 10 045003

[2]. Vetter RJ, Williams JC, Hetke JF, Nunamaker EA and Kipke DR 2004 Chronic neural recording using silicon-substrate microelectrode arrays implanted in cerebral cortex IEEE Trans. Biomed. Eng. 51 896–904 [PubMed: 15188856]

[3]. Badia J, Raspopovic S, Carpaneto J, Micera S and Navarro X 2016 Spatial and functional selectivity of peripheral nerve signal recording with the transversal intrafascicular multichannel electrode (TIME) IEEE Trans. Neural Syst. Rehabil. Eng. 24 20–27 [PubMed: 26087496]

[4]. Hochberg LR et al. 2006 Neuronal ensemble control of prosthetic devices by a human with tetraplegia Nature 442 164–71 [PubMed: 16838014]

[5]. George JA et al. 2020 Long-term performance of Utah slanted electrode arrays and intramuscular electromyographic leads implanted chronically in human arm nerves and muscles J. Neural Eng. 17 056042

[6]. Barrese JC et al. 2013 Failure mode analysis of silicon-based intracortical microelectrode arrays in non-human primates J. Neural Eng. 10 066014

[7]. McCreery DB, Agnew WF, Yuen TGH and Bullara L 1990 Charge density and charge per phase as cofactors in neural injury induced by electrical stimulation IEEE Trans. Biomed. Eng. 37 996–1001 [PubMed: 2249872]

[8]. Cogan SF, Ludwig KA, Welle CG and Takmakov P 2016 Tissue damage thresholds during therapeutic electrical stimulation J. Neural Eng. 13 021001

[9]. Gunter C, Delbeke J and Ortiz-Catalan M 2019 Safety of long-term electrical peripheral nerve stimulation: review of the state of the art J. Neuroeng. Rehabil. 16 13 [PubMed: 30691482]

[10]. Cogan SF 2008 Neural stimulation and recording electrodes Annu. Rev. Biomed. Eng. 10 275–309 [PubMed: 18429704]

[11]. Hu Z, Troyk P, DeMichele G, Kayvani K and Suh S 2012 Intrinsic activation of iridium electrodes over a wireless link 34th Annual Int. Conf. IEEE EMBS (San Diego, CA) pp 2788–91

[12]. Frederick RA, Meliane IY, Joshi-Imre A, Troyk PR and Cogan SF 2020 Activated iridium oxide film (AIROF) electrodes for neural tissue stimulation J. Neural Eng. 17 056001

[13]. Troyk PR and DeMichele GA 2003 Inductively-coupled power and data link for neural prostheses using a class-E oscillator and FSK modulation Proc. 25th Annual Int. Conf. IEEE Engineering in Medicine and Biology Society (IEEE Cat No03CH37439) (17–21 September 2003) (10.1109/IEMBS.2003.1280869)

[14]. Rush A, Suh S and Troyk PR 2011 An inductive link for an intracortical visual prosthesis IEEE EMBS Conf. Neural Engineering (Cancun, Mexico) (10.1109/NER.2011.5910596)

[15]. Rush A and Troyk PR 2011 Dual inductive link coil design for a neural recording system 2011 Annual Int. Conf. IEEE Engineering in Medicine and Biology Society 30–3 August–September 2011 (10.1109/IEMBS.2011.6091579)

[16]. Rush AD and Troyk PR 2012 A power and data link for a wireless-implanted neural recording system IEEE Trans. Biomed. Eng. 59 3255–62 [PubMed: 22922687]

[17]. Troyk PR, Detlefsen DEA and DeMichele GAD 2006 A multifunctional neural electrode stimulation ASIC using Neurotalk™ interface 2006 Int. Conf. IEEE Engineering in Medicine and Biology Society 30–3 August–September 2006 (10.1109/IEMBS.2006.260630)

[18]. Yoo JM, Negi S, Tathireddy P, Solzbacher F, Song JI and Rieth LW 2013 Excimer laser deinsulation of Parylene-C on iridium for use in an activated iridium oxide film-coated Utah electrode array J. Neurosci. Methods 215 78–87 [PubMed: 23458659]

[19]. Cogan SF, Troyk PR, Ehrlich J, Plante TD and Detlefsen DE 2006 Potential-biased, asymmetric waveforms for charge-injection with activated iridium oxide (AIROF) neural stimulation electrodes IEEE Trans. Biomed. Eng. 53 327–32 [PubMed: 16485762]

[20]. Deuis JR, Dvorakova LS and Vetter I 2017 Methods used to evaluate pain behaviors in rodents Front. Mol. Neurosci. 10 284 [PubMed: 28932184]

[21]. Metz GA and Whishaw IQ 2009 The ladder rung walking task: a scoring system and its practical application J. Vis. Exp. 28 e1204

[22]. Nowicki M et al. 2014 Effects of isoflurane anesthesia on F-waves in the sciatic nerve of the adult rat Muscle Nerve 50 257–61 [PubMed: 24347162]

[23]. Sotocinal SG et al. 2011 The Rat Grimace Scale: a partially automated method for quantifying pain in the laboratory rat via facial expressions Mol. Pain 7 55 [PubMed: 21801409]

[24]. Frederick RA, Troyk PR and Cogan SF 2020 Selective wireless stimulation of rat sciatic nerve* 2020 42nd Annual Int. Conf. IEEE Engineering in Medicine & Biology Society (EMBC) 20–24 July 2020 (10.1109/EMBC44109.2020.9175335)

[25]. Bredeson S, Kanneganti A, Deku F, Cogan S, Romero-Ortega M and Troyk P 2015 Chronic in-vivo testing of a 16-channel implantable wireless neural stimulator 2015 37th Annual Int. Conf. of the IEEE Engineering in Medicine and Biology Society (EMBC) vol 2015 pp 1017–20

[26]. Troyk P et al. 2015 In-vivo tests of a 16-channel implantable wireless neural stimulator 2015 7th Int. IEEE/EMBS Conf. Neural Engineering (NER) 22–24 April 2015 (10.1109/NER.2015.7146662)

[27]. Badia J, Pascual-Font A, Vivo M, Udina E and Navarro X 2010 Topographical distribution of motor fascicles in the sciatic-tibial nerve of the rat Muscle Nerve 42 192–201 [PubMed: 20544926]

[28]. Branner A and Normann RA 2000 A multielectrode array for intrafascicular recording and stimulation in sciatic nerve of cats Brain Res. Bull. 51 293–306

[29]. Branner A, Stein RB, Fernandez E, Aoyagi Y and Normann RA 2004 Long-term stimulation and recording with a penetrating microelectrode array in cat sciatic nerve IEEE Trans. Biomed. Eng. 51 146–57

[30]. Mathews KS, Wark HA and Normann RA 2014 Assessment of rat sciatic nerve function following acute implantation of high density Utah slanted electrode array (25 electrodes/mm(2)) based on neural recordings and evoked muscle activity Muscle Nerve 50 417–24 [PubMed: 24638985]

[31]. Polasek KH, Hoyen H, Keith MW, Kirsch RF and Tyler DJ 2009 Stimulation stability and selectivity of chronically implanted multicontact nerve cuff electrodes in the human upper extremity IEEE Trans. Neural Syst. Rehabil. Eng. 17 428–37

[32]. Fisher LE, Tyler DJ, Anderson JS and Triolo RJ 2009 Chronic stability and selectivity of four-contact spiral nerve-cuff electrodes in stimulating the human femoral nerve J. Neural Eng. 6 046010

[33]. Freeberg MJ, Pinault GCJ, Tyler DJ, Triolo RJ and Ansari R 2020 Chronic nerve health following implantation of femoral nerve cuff electrodes J. Neuroeng. Rehabil. 17 95 [PubMed: 32664972]

[34]. Schiefer MA et al. 2013 Selective activation of the human tibial and common peroneal nerves with a flat interface nerve electrode J. Neural Eng. 10 056006

[35]. Delianides C, Tyler D, Pinault G, Ansari R and Triolo R 2020 Implanted high density cuff electrodes functionally activate human tibial and peroneal motor units without chronic detriment to peripheral nerve health Neuromodulation 23 754–62 [PubMed: 32189421]

[36]. Tan DW, Schiefer MA, Keith MW, Anderson JR and Tyler DJ 2015 Stability and selectivity of a chronic, multi-contact cuff electrode for sensory stimulation in human amputees J. Neural Eng. 12 026002

[37]. Biran R, Martin DC and Tresco PA 2007 The brain tissue response to implanted silicon microelectrode arrays is increased when the device is tethered to the skull J. Biomed. Mater. Res. A 82 169–78 [PubMed: 17266019]

[38]. Vasudevan S, Patel K and Welle C 2017 Rodent model for assessing the long term safety and performance of peripheral nerve recording electrodes J. Neural Eng. 14 016008

[39]. Perry J and Burnfield JM 2010 Gait Analysis: Normal and Pathological Function 2nd edn (Thorofare, NJ: SLACK Incorporated)

[40]. Frederick RA, Margolis R, Hoyt K and Cogan SF 2020 Evaluating microelectrode arrays in peripheral nerve using micro computed tomography∗ 2020 42nd Annual Int. Conf. IEEE Engineering in Medicine & Biology Society (EMBC) 20–24 July 2020 (10.1109/EMBC44109.2020.9176598)

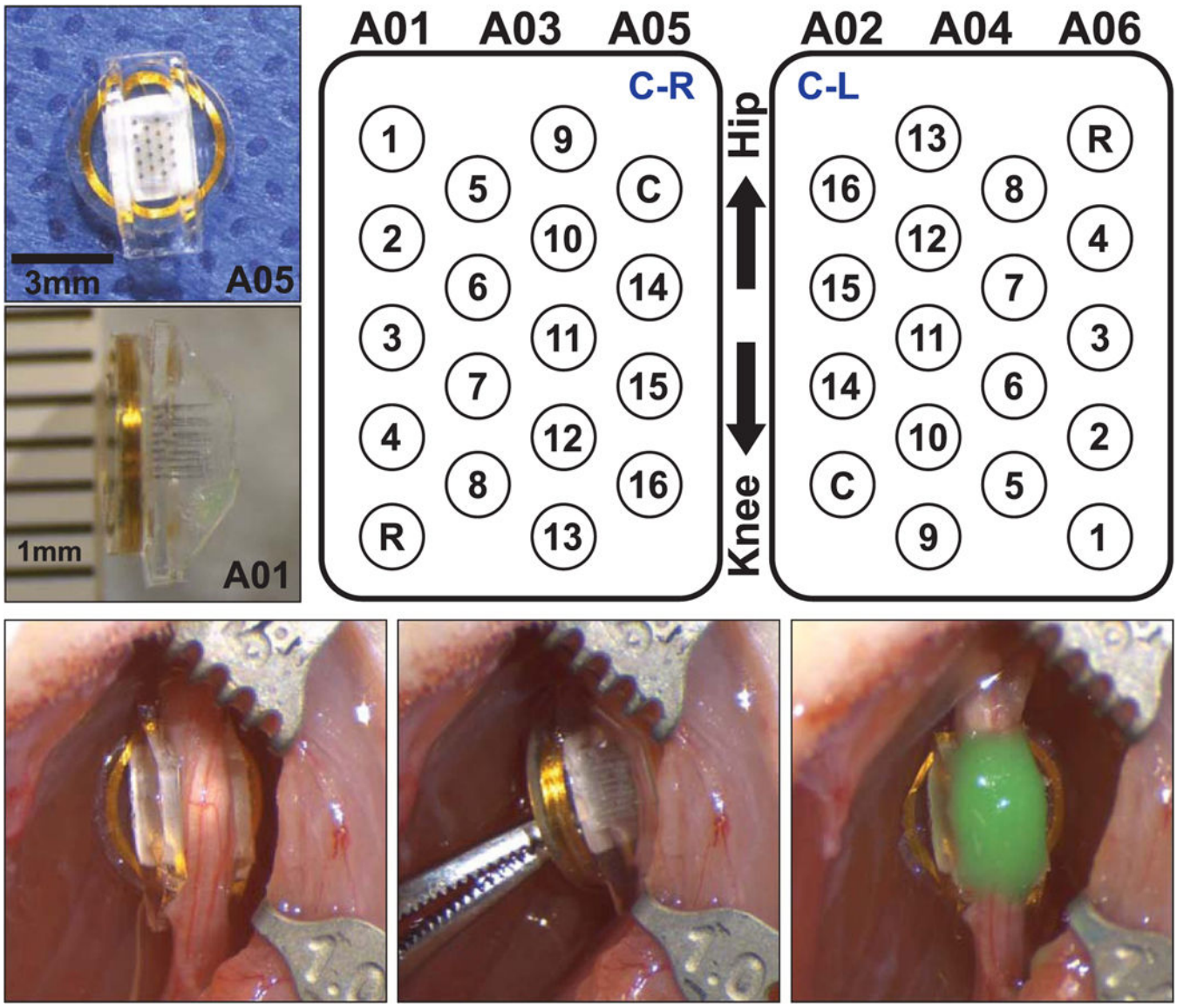

Figure 1.

(Top left) Images of the WFMA device before implantation in animal A05 and after explant from animal A01. (Top right) Electrode array layout showing device orientations 'C-R' and 'C-L' when implanted on the nerve as viewed from above, looking down into the silicone channel. Locations of the reference and counter electrodes are indicated by R and C, respectively. (Bottom) WFMA device in the left sciatic nerve of animal A06 after inserting the electrodes and after securing the WFMA with silicone sealant (Kwik-Cast™).

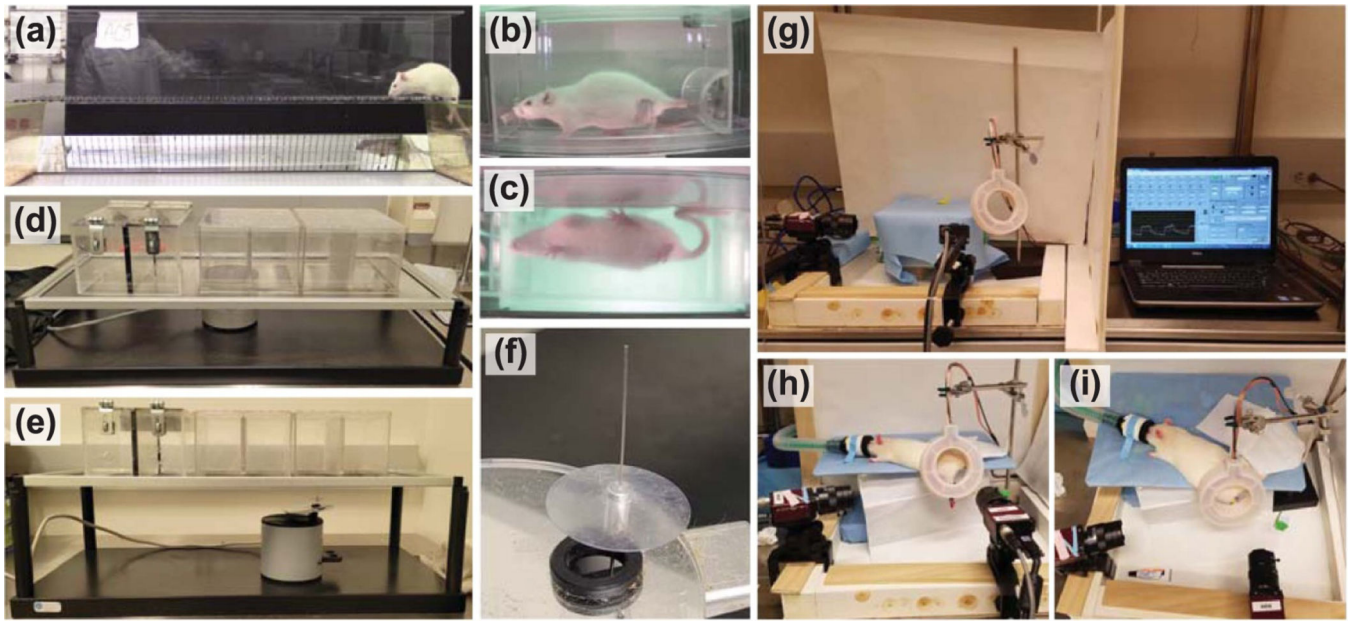

Figure 2.

Equipment and set-up for 38 week study assessments. (a) Ladder walking trials. Still frame from video recording of animal A05, post-implantation week 38. (b) and (c) Treadmill walking trials side view and bottom mirror view, respectively. Still frames from video recording of animal A06, post-implantation week 2. (d) Hargraeve's apparatus for testing response to thermal stimulus. (e) and (f) Plantar aesthesiometer set-up and 5 mm filament for testing response to pressure stimulus. (g) Equipment and control graphical user interface for investigating response to sciatic nerve stimulation. (h) Side view and (i) top view of animal A01 with external telemetry coil positioned over the implanted WFMA during stimulation tests with video recording under isoflurane anesthesia.

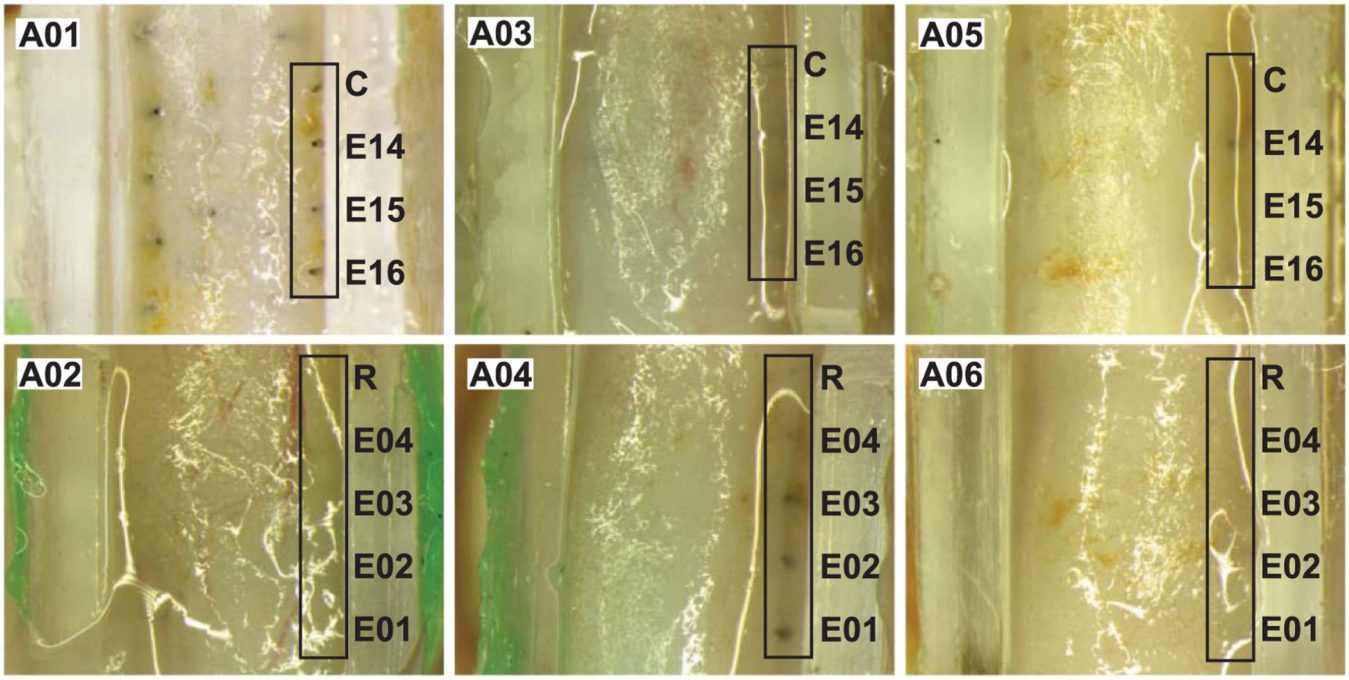

Figure 3.

End-of-study electrode assessment showing a top-down view into the silicone guide channel. Each image shows the gross position of electrodes at the outer edge of the sciatic nerve for each implanted animal subject (A01, A02, A03, A04, A05, A06). Images were taken after removal of the green silicone sealant covering the nerve, after fixation and removal of the sciatic nerve at post-implantation week 38.

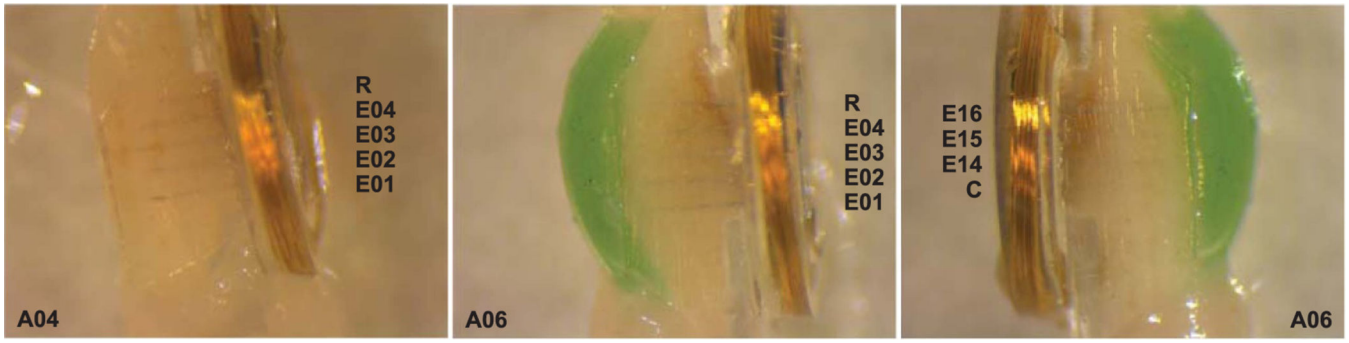

Figure 4.

End-of-study electrode assessment showing side views into the silicone guide channel. Proximal end of the nerve is positioned towards the top of the image and distal end towards the bottom. (Left) Right side of electrode array removed from animal A04. (Middle) Right side of electrode array removed from animal A06. (Right) Left side of electrode array removed from animal A06. Images were taken after fixation and removal of the sciatic nerve from the animal at post-implantation week 38.

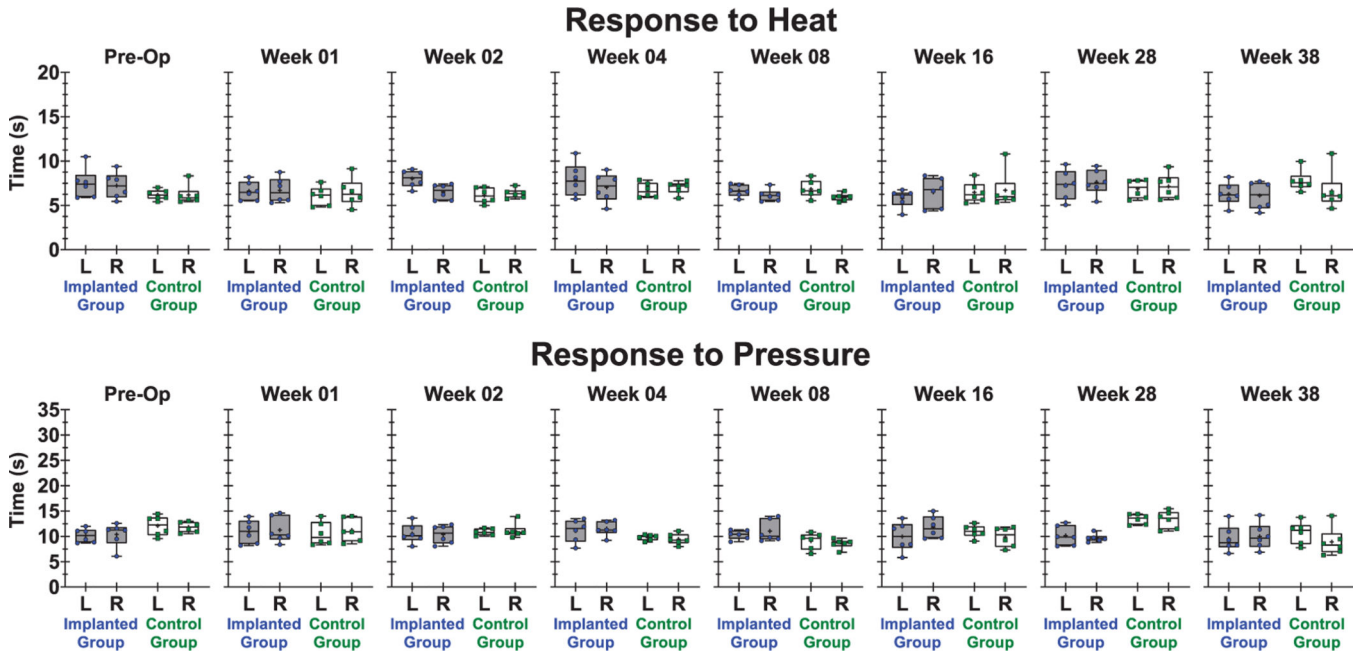

Figure 5.

Time to paw withdrawal in response to sensory stimuli for selected time points pre-op and post-op weeks 1, 2, 4, 8, 16, 28, and 38. (Top) Response to heat and (bottom) response to pressure, where data points within the box plots represent each animal in the implanted group or control group and the mean of $n = 6$ animals is indicated by the (+) symbol. Data within each group are separated by rear left (L) or rear right (R) paw.

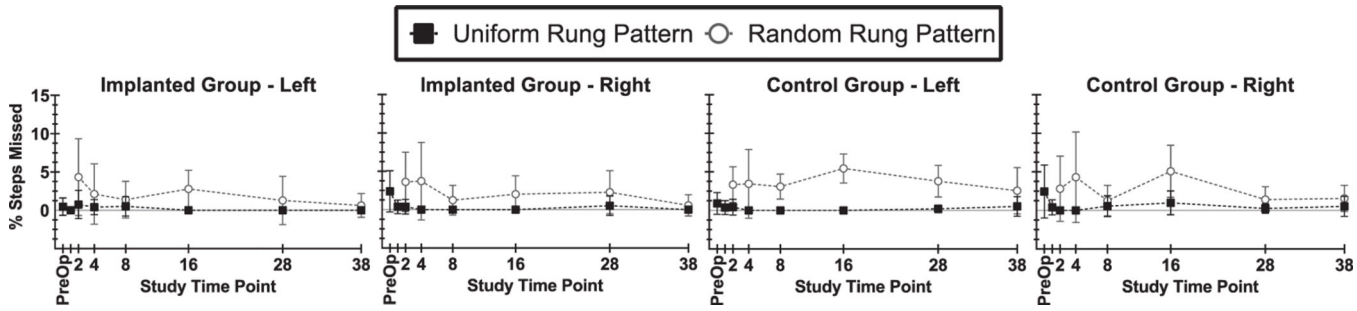

Figure 6.

Percentage of missed steps in ladder walking trials for selected time points pre-op and post-op weeks 1, 2, 4, 8, 16, 28, and 38.

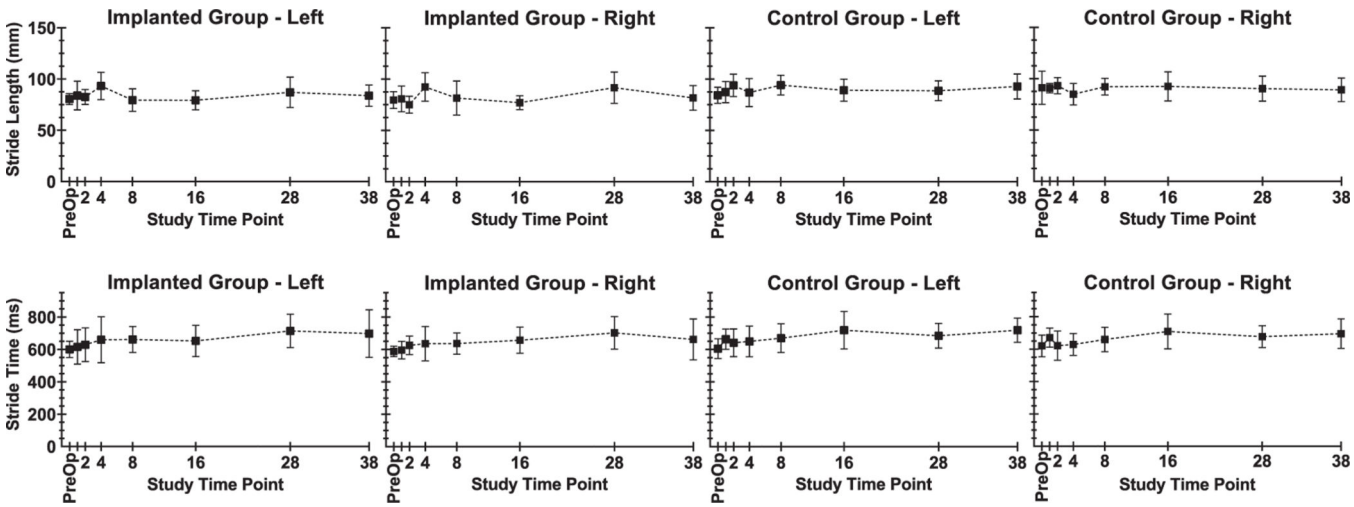

Figure 7.

Step length and step time parameters from treadmill walking trials for selected time points pre-op and post-op weeks 1, 2, 4, 8, 16, 28, and 38.

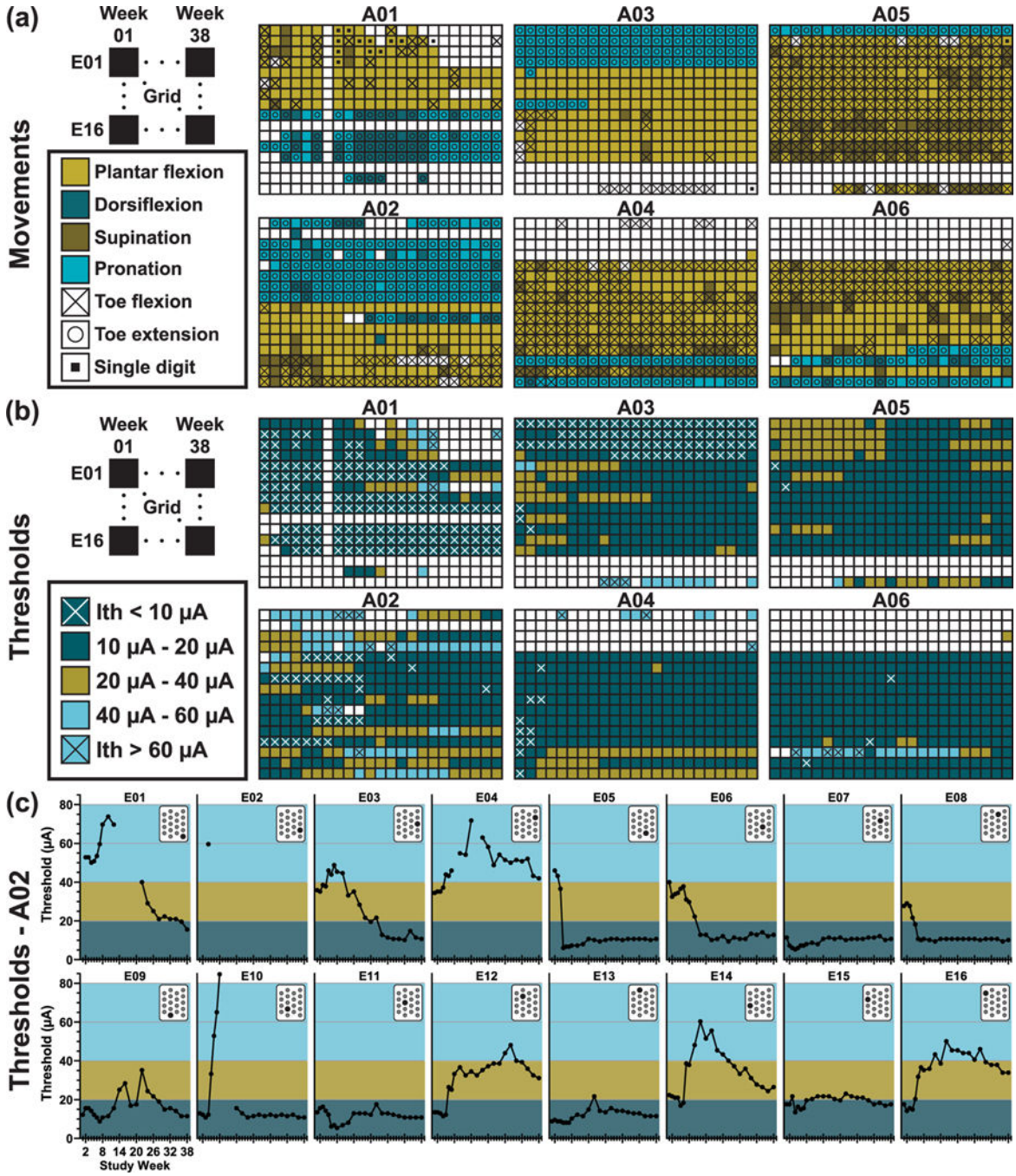

Figure 8.

(a) Maps of limb motion observed in response to stimulation. Rows represent each of the 16 electrodes in the implanted array and columns represent each time point of recorded data (week 1, 2, 3, 4, 5, 6, 7, 8, 10, 12, 14, 16, 18, 20, 22, 24, 26, 28, 30, 32, 34, 36, 38). For animal A01, no data was recorded during week 7, and no data was recorded for electrode 10 at any time point as the electrode was determined to be non-functional at the time of device fabrication. (b) Color maps of the current threshold values required to generate visible movement in the implanted limb (Implanted Group—left hindlimb). Rows represent each of

the 16 electrodes in the implanted array and columns represent each time point of recorded data (week 1, 2, 3, 4, 5, 6, 7, 8, 10, 12, 14, 16, 18, 20, 22, 24, 26, 28, 30, 32, 34, 36, 38). For animal A01, no data was recorded during week 7, and no data was recorded for electrode 10 at any time point as the electrode was determined to be non-functional at the time of device fabrication. (c) Current thresholds over time for each separate electrode implanted in animal A02. Position of the electrode is indicated in the array layout shown in the upper right corner of each graph.

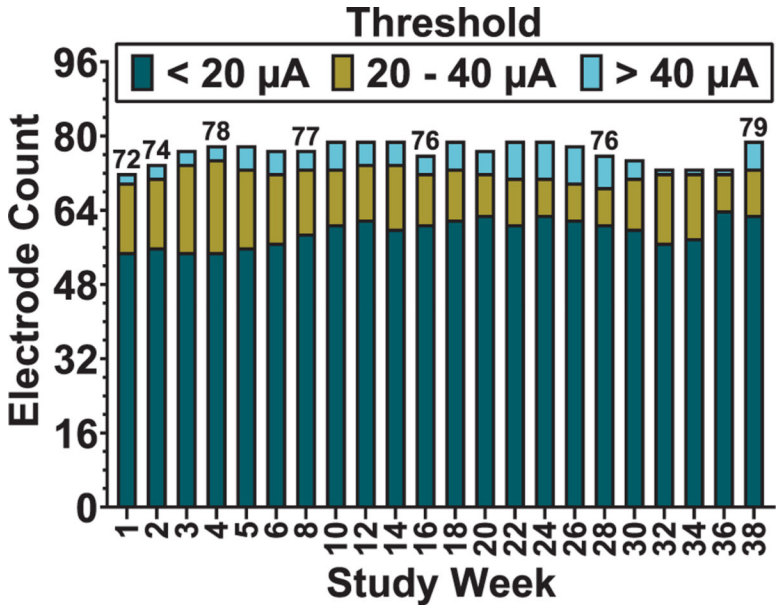

Figure 9.

Total number of electrodes (n = 6 animals) evoking movement at all tested time points during the study. Each count is broken down into the number of electrodes generating movement within three different current threshold ranges, 0–20 μA (dark blue), 20–40 μA (gold), and above 40 μA (light blue).

Table 1.

Animal groups and device orientation.

Animal ID	Device ID	Orientation	Animal ID	Device ID	Orientation
A01	W00REB01–65	C-R	B01	No implant	N/A
A02	W002D-60–2	C-L	B02	No implant	N/A
A03	W003D-61–3	C-R	B03	No implant	N/A
A04	W004D-62–4	C-L	B04	No implant	N/A
A05	W0005–11-05	C-R	B05	No implant	N/A
A06	W0006–21-09	C-L	B06	No implant	N/A

Table 2.

Average step scores from ladder walking task.

Study	Implanted Group Rear Left		Implanted Group Rear Right		Control Group Rear Left		Control Group Rear Right	
Timepoint	Uniform	Random	Uniform	Random	Uniform	Random	Uniform	Random
Pre-op	5.4 ± 0.1		5.3 ± 0.1		5.4 ± 0.1		5.3 ± 0.1	
Week 01	5.4 ± 0.1		5.4 ± 0.1		5.3 ± 0.2		5.3 ± 0.2	
Week 02	5.4 ± 0.2	5.2 ± 0.4	5.5 ± 0.1	5.3 ± 0.3	5.3 ± 0.3	5.1 ± 0.2	5.2 ± 0.3	5.1 ± 0.2
Week 04	5.4 ± 0.2	5.1 ± 0.4	5.3 ± 0.2	5.2 ± 0.4	5.5 ± 0.1	5.4 ± 0.3	5.4 ± 0.2	5.3 ± 0.3
Week 08	5.2 ± 0.2	5.1 ± 0.2	5.2 ± 0.2	5.1 ± 0.3	5.3 ± 0.1	5.3 ± 0.2	5.3 ± 0.1	5.3 ± 0.2
Week 16	5.3 ± 0.2	5.2 ± 0.2	5.3 ± 0.2	5.3 ± 0.2	5.4 ± 0.1	5.2 ± 0.2	5.4 ± 0.1	5.1 ± 0.3
Week 28	5.3 ± 0.2	5.2 ± 0.4	5.2 ± 0.2	5.1 ± 0.4	5.4 ± 0.1	5.3 ± 0.3	5.4 ± 0.1	5.4 ± 0.1
Week 38	5.3 ± 0.3	5.2 ± 0.4	5.3 ± 0.2	5.3 ± 0.4	5.4 ± 0.1	5.3 ± 0.2	5.5 ± 0.1	5.4 ± 0.2